Compensatory Genetic and Transcriptional Cytonuclear Coordination in Allopolyploid Lager Yeast (*Saccharomyces pastorianus*)

Keren Zhang [1,†] Juzuo Li [1,†] Guo Li,[1,†] Yue Zhao,[1] Yuefan Dong,[1] Ying Zhang,[1] Wenqing Sun,[1] Junsheng Wang,[1] Jinyang Yao,[1] Yiqiao Ma,[2] Hongyan Wang,[3] Zhibin Zhang,[1] Tianya Wang,[1] Kun Xie,[1] Jonathan F. Wendel [4] Bao Liu [1,*] and Lei Gong [1,*]

[1]Key Laboratory of Molecular Epigenetics of the Ministry of Education (MOE), Northeast Normal University, Changchun, Jilin 130024, China

[2]Jilin Academy of Vegetable and Flower Science, Changchun, Jilin 130033, China

[3]Laboratory of Plant Epigenetics and Evolution, School of Life Science, Liaoning University, Shenyang, Liaoning 110036, China

[4]Department of Ecology, Evolution and Organismal Biology, Iowa State University, Ames, IA 50010, USA

[†]These authors contributed equally to this work.

***Corresponding authors:** E-mail: baoliu@nenu.edu.cn; gongl100@nenu.edu.cn.

Associate editor: Dr Patricia Wittkopp

Abstract

Cytonuclear coordination between biparental-nuclear genomes and uniparental-cytoplasmic organellar genomes in plants is often resolved by genetic and transcriptional cytonuclear responses. Whether this mechanism also acts in allopolyploid members of other kingdoms is not clear. Additionally, cytonuclear coordination of interleaved allopolyploid cells/individuals within the same population is underexplored. The yeast *Saccharomyces pastorianus* provides the opportunity to explore cytonuclear coevolution during different growth stages and from novel dimensions. Using *S. pastorianus* cells from multiple growth stages in the same environment, we show that nuclear mitochondria-targeted genes have undergone both asymmetric gene conversion and growth stage-specific biased expression favoring genes from the mitochondrial genome donor (*Saccharomyces eubayanus*). Our results suggest that cytonuclear coordination in allopolyploid lager yeast species entails an orchestrated and compensatory genetic and transcriptional evolutionary regulatory shift. The common as well as unique properties of cytonuclear coordination underlying allopolyploidy between unicellular yeasts and higher plants offers novel insights into mechanisms of cytonuclear evolution associated with allopolyploid speciation.

Key words: **cytonuclear coevolution, allotetraploid lager yeast, nuclear mitochondria-targeted gene.**

Article

Introduction

Polyploidy, or whole-genome duplication (WGD), is ubiquitous across eukaryotic kingdoms (Jiao et al. 2011; Choleva and Janko 2013; Soltis et al. 2015; Rodriguez and Arkhipova 2018), and has been important in fungal evolution (Albertin and Marullo 2012; Todd et al. 2017; Gorkovskiy and Verstrepen 2021; Marsit et al. 2021). Polyploidy also is known to have contributed to rapid adaptation and increase species diversity during the evolutionary history of the representative model budding yeast genus *Saccharomyces* (Selmecki et al. 2015). It is possible to analyze the genetic and transcriptional responses to WGD using autopolyploid (polyploids with multiple chromosome sets derived from a single taxon) or allopolyploid (polyploids with chromosomes derived from two or more diverged taxa) yeasts (Krogerus et al. 2016; Scott et al. 2017).

Lager yeast (*Saccharomyces pastorianus*) is a well described, naturally evolved allopolyploid species that has been utilized for many centuries for bottom fermentation at low temperatures to produce lager beers (Nakao et al. 2009). Both allotriploid and allotetraploid lager yeasts have been identified (Monerawela and Bond 2018; Salazar et al. 2019). Previous work has suggested that the closest extant relatives of the allopolyploid genome donors to *S. pastorianus* involve strain(s) of *Saccharomyces cerevisiae* and an *Saccharomyces eubayanus* strain from Tibet (Libkind et al. 2011; Bing et al. 2014), with the mitochondrial donor being closely related to the Tibetan *S. eubayanus* strain (Okuno et al. 2016). There is a well-annotated mitochondrial genome of *S. eubayanus* (Baker et al. 2015), which is about 22 kb smaller (64.0 kb) than the 85.8 kb mitochondrial genome of *S. cerevisiae*. Together with a recent chromosome-level genome assembly of lager yeast (*S. pastorianus* CBS 1483; Salazar et al. 2019), this

system provides the genomic resources necessary for studying mitochondrial genes and identifying subgenomic nuclear homoeologs (genes duplicated via polyploidy) within allopolyploid lager yeasts.

Similar to allopolyploid plant species, allopolyploid lager yeasts need to overcome cytonuclear challenges accompanying the merger of nuclear genomes from two species with the organellar genome from only one (Gong et al. 2012, 2014; Barnard-Kubow et al. 2017; Sloan et al. 2018; Li et, al. 2019, 2020; Timouma et al. 2021; Forsythe et al. 2022; Sharbrough et al. 2022). Taking allopolyploid lager yeasts as an example, the combination of divergent *S. cerevisiae* and *S. eubayanus* nuclear genomes but the inheritance of only *S. eubayanus* progenitor organellar mitochondrial genome could result in a challenge of coordination between mitochondrial-targeted *S. cerevisiae* homoeologs and the *S. eubayanus* mitochondria. Identification of fertility-related mitochondrial genes in the nuclear genome of hybrid (*S. cerevisiae* and *S. eubayanus*) yeast reflects the importance of mitochondrial–nuclear compatibility in yeast speciation (Lee et al. 2008; Solieri 2010; Leducq et al. 2017). Studies focusing on the *rbcS*-encoding, chloroplast-targeted small subunits of RuBisCo have characterized cytonuclear processes accompanying allopolyploid evolution in angiosperms (Gong et al. 2012, 2014; Wang et al. 2017). One characterized route reducing potential cytonuclear conflict is intergenomic homogenization of *rbcS* homoeologs through "paternal-to-maternal" gene conversions (Gong et al. 2014; Li et al. 2019, 2020; Grover et al. 2022). At the transcriptional level, a second path involves biased expression of *rbcS* homoeologs in the direction predicted by the organellar origin in the allopolyploids (Gong et al. 2012, 2014; Wang et al. 2017). These and other coordinated cytonuclear responses are thought to stabilize or optimize RuBisCo holoenzyme activity.

Population growth in allotetraploid lager yeasts can be divided into four characteristic stages or phases, namely, lagging, exponential/log, stationary, and death, and are monitored by optical absorbance densities at 600 nm (short OD_{600}). Similar to other microbial populations, *Saccharomyces* species exhibit unique physical and metabolic states across these different stages or phases (Johnson 1968; Ginovart et al. 2011, 2018; Olivares-Marin et al. 2018). For example, rapid multiplication of cells and consumption of sugar occur in the exponential/log phase, whereas the subsequent stationary phase involves flocculation (the act of yeasts aggregating into "clumps") and preparation for nutritional constraints (i.e., running out of sugar supply). These characteristic population level features allow us to explore transcriptomic cytonuclear responses that characterize each specific phase. Importantly, allopolyploid yeasts living in the same habitat are interconnected via multiple metabolic and physiological routes, and thus individuals are not really independent (MacLean and Gudelj 2006; Bleoanca et al. 2013; Youk and Lim 2014; Laman Trip and Youk 2020). These interactions integrate the allopolyploid yeast individuals into an interleaved population, representing an interesting model for exploring cytonuclear coordination at the population level in the same habitat.

In the present study, we describe genome-wide cytonuclear coevolution for nuclear mitochondria-targeted (hereafter abbreviated as NMT) genes in fungal allopolyploid yeasts. We identified homologous NMT groups in allopolyploid *S. pastorianus* and models of its diploid genome donors *S. cerevisiae* and *S. eubayanus*. Based on the finding that the NMT homoeologs in *S. pastorianus* were under strong purifying selection, we characterized genomic and transcriptional coordination during microaerobic growth stages. Our work shows that cytonuclear evolutionary responses to allopolyploidy in lager yeasts bear similarities to those of plants, comprising both unidirectional homoeologous gene conversions and biased expression for homoeologs of *S. eubayanus* origin. Our findings provide novel insights into the general and unique features of cytonuclear coevolution in unicellular fungal allopolyploid species.

Results

NMT Genes are Under Strong Purifying Selection Pressure Conveyed from Cytoplasmic Mitochondria of *Saccharomyces eubayanus* Origin

Allopolyploid *Saccharomyces pastorianus* originated through complex hybridization events (allotriploidization and allotetraploidization), involving progenitors similar to modern *S. eubayanus* and *S. cerevisiae*. Based on the aligned ORFs of coding genes in mitochondrial DNAs (hereafter mtDNAs), mtDNAs maintained in *S. pastorianus* were confirmed to be inherited from the *S. eubayanus*-like parent (Okuno et al. 2016). To increase the resolution of phylogenetic analysis, we compared whole-genomic mtDNA SNPs (in both coding and non-coding regions) in all yeast strains studied to confirm the mitochondrial origin of our *S. pastorianus* strains. The phylogenetic placement of all *S. pastorianus* mtDNAs as sister to *S. eubayanus* confirms that the mitochondrial genomes of all three allopolyploid *S. pastorianus* strains were indeed contributed by *S. eubayanus* (supplementary fig. S1, Supplementary Material online).

Allopolyploid *S. pastorianus* exhibits low-temperature tolerance, enabled by its mitochondrial DNA inherited from cryotolerant *S. eubayanus* (Baker et al. 2015). Accordingly, it is hypothesized that specific mitochondrial genes (mtDNA genes) in both diploid *S. eubayanus* and allopolyploid *S. pastorianus* could be under selection for cold tolerance. In addition, considering the importance of NMT genes in mitochondrial activities (Bousquet et al. 1991; Malina et al. 2018), it is reasonable to hypothesize that selection also acts on NMT genes in cryotolerant yeasts as well. To test these hypotheses, we characterized mtDNA genes, non-NMT, and NMT homolog groups in both diploid *S. eubayanus* and allopolyploid *S. pastorianus*. Based upon sequence alignments of each gene homolog group, we estimated and compared their ratios of

nonsynonymous to synonymous substitutions (d_N/d_S ratios) between species at the same and different ploidy levels and even between subgenomes within the same allopolyploid species.

In both diploid *S. eubayanus* and allopolyploid *S. pastorianus*, all genes except *atp8* harbored d_N/d_S ratios less than 1.0, consistent with purifying selection (fig. 1A; supplementary table S2, Supplementary Material online). *atp8* was an outlier with a high d_N/d_S ratio resulting from its single nonsynonymous substitution. Importantly, the *cox1* gene with a lower d_N/d_S ratio had a specific allele type which was confirmed to confer cryotolerance in *Saccharomyces uvarum* (Li et al. 2019). For the profiles of NMT and non-NMT genes in the genomes of diploid *S. cerevisiae*, *S. eubayanus*, and allopolyploid *S. pastorianus* strain(s) were characterized by sequence similarity searches against genes in the fungal secretome and subcellular proteome knowledgebase (Meinken et al. 2014) (table 1), in which mitochondria-targeted is well annotated. A total of 1616 (26.90%) NMT and 4392 (73.10%) non-NMT genes were identified in *S. cerevisiae*, whereas 535 (9.95%) NMT and 4842 (90.05%) non-NMT genes were identified in *S. eubayanus* (table 1). In principle, the differences in the abundance of NMT genes in *S. cerevisiae* and *S. eubayanus* could reflect differences in qualities of their genome assemblies/annotations and/or to actual evolutionary divergence in NMT gene composition in yeast species or strains. Given the numbers and relative abundances of NMT genes in the two subgenomes C (*S. cerevisiae* contributed; 871 [23.09%], 1261 [23.04%], and 1365 [23.94%] genes) and E (*S. eubayanus* contributed; 456 [9.30%], 429 [9.15%], and 465 [9.26%] genes) in multiple *S. pastorianus* allopolyploid strains (table 1), we infer that the difference is real rather than due to annotation or genome assembly issues. Notably, the significantly higher abundance of NMT genes (or lower abundance of non-NMT genes) in *S. cerevisiae* than those in both *S. eubayanus* and the C subgenome of *S. pastorianus* (Proportion test, P value < 0.01; table 1) and absence of this pattern in *S. eubayanus* and the E subgenome of *S. pastorianus* (Proportion test, P value > 0.05; table 1) implicate either amplification in the number of NMT genes in *S. cerevisiae* or genome-wide loss of genes in *S. pastorianus*, consistent with their differences in genome size (85.8 vs 68.6 kb).

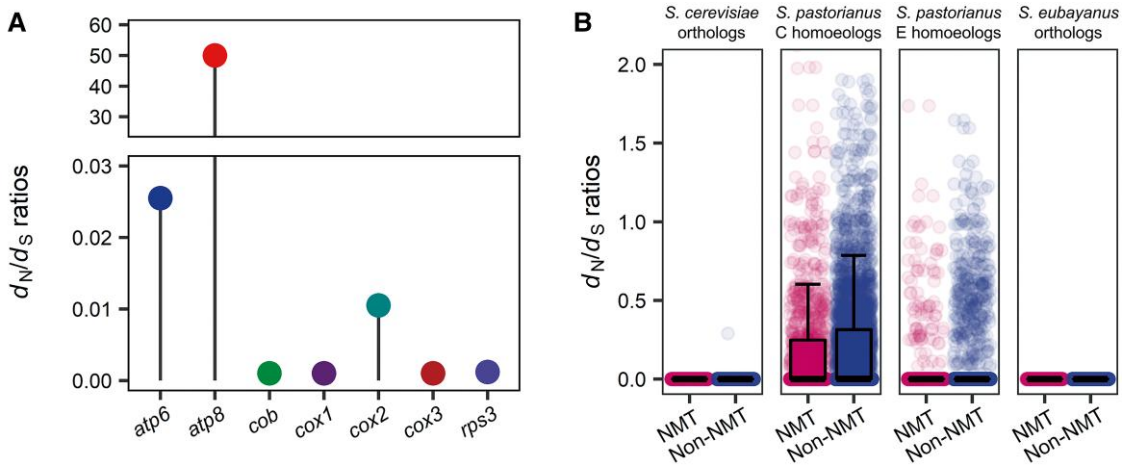

Fig. 1. Nonsynonymous to synonymous substitution ratios (d_N/d_S) of mitochondrial and nuclear genes. (*A*) d_N/d_S ratios (*y*-axis) of homologous mitochondrial genes (mtDNA genes; *x*-axis) in *S. pastorianus* and *S. eubayanus* are summarized; (*B*) Each panel summarizes the d_N/d_S ratios of all single-copy NMT and non-NMT genes characterized in diploid orthologs of *S. eubayanus* and *S. cerevisiae* and subgenomic homoeologs of allopolyploid *S. pastorianus*.

Table 1. The Number of NMT and Non-NMT Genes Identified in Diploid and Allopolyploid Yeast Strains.

Species		Type	NMT		Non-NMT	
S. pastorianus	**CBS 1513**	**C**[a]	**871**	**23.09%**	**2901**	**76.91%**
		E[a]	**456**	**9.30%**	**4445**	**90.70%**
	WS 34/70	**C**	**1261**	**23.04%**	**4212**	**76.96%**
		E	**429**	**9.15%**	**4262**	**90.85%**
	CBS 1483	**C**	**1365**	**23.94%**	**4336**	**76.06%**
		E	**465**	**9.26%**	**4554**	**90.74%**
S. cerevisiae	**FostersO**	**Ale**	**1616**	**26.90%**	**4392**	**73.10%**
	NCYC1063	**Stout**	**1616**	**26.90%**	**4392**	**73.10%**
S. eubayanus	**CDFM21L.1**	**Tibetan**	**535**	**9.95%**	**4842**	**90.05%**

The bold values represent the relative proportion of NMT or Non-NMT genes within each diploid or polyploid subgenome.
[a]C and E represent the *S. cerevisiae*- and *S. eubayanus*-subgenomes in *S. pastorianus*, respectively.

Interestingly, the number of NMT and non-NMT genes varied across different allopolyploid *S. pastorianus* strains, with fewer C subgenomic NMT and non-NMT genes in the CBS 1513 strain (871 [23.09%] and 2901 [76.91%], respectively). To minimize potential artifactual (genome assembly/annotation) effects, we grouped single-copy biparental diploid orthologs with their respective subgenomic homoeologous copies (all homologs exist in single-copy status) for each allopolyploid *S. pastorianus* strain into a homolog group by OrthoFinder (Emms and Kelly 2019). These single-copy, homologous NMT and non-NMT gene groups were input into subsequent evolutionary analyses (table 2).

We compared d_N/d_S ratios for diploid orthologs and their respective C and E subgenomic homoeologs within each NMT and non-NMT gene group as well (fig. 1*B*; supplementary table S3, Supplementary Material online). Of note, for parental diploid orthologs, the d_N/d_S ratios of most NMT and non-NMT genes were zero (fig. 1*B*), implicating a dominant pattern of purification selection. After allopolyploidy, within both NMT and non-NMT gene groups, d_N/d_S ratios of C subgenomic homoeologs were significantly higher than those of E subgenomic copies (fig. 1*B*). Intriguingly, for E subgenomic homoeologs, most d_N/d_S ratios of NMT and non-NMT homoeologs were less than 1.0 while ratios of NMT group were lower than those of the non-NMT group (Wilcoxon Rank Sum test, P value < 0.01); as for C subgenomic homoeologs, most d_N/d_S ratios of NMT homoeologs were still less than 1.0 while there were more non-NMT homoeologs harboring d_N/d_S ratios higher than 1.0, which make the former ratios significantly lower than the latter (fig. 1*B*). These observations indicate that both E and C subgenomic NMT homoeologs in *S. pastorianus* were still under purifying selection from cytoplasmic mitochondria of *S. eubayanus* origin whereas selective constraints for E subgenomic NMT homoeologs are higher than for C subgenomic NMT copies.

Table 2. Single-Copy NMT and Non-NMT Gene Groups in Diploid and Allopolyploid *Saccharomyces* Strains.

Group Names	Member		Number of Groups		
			NMT	Non-NMT	Total
CBS 1513 group	*S. pastorianus*	CBS 1513	682	2152	2834
	S. cerevisiae	FostersO			
	S. eubayanus	NCYC 1063 CDFM21L.1			
WS 34/70 group	*S. pastorianus*	WS 34/70	971	3015	3986
	S. cerevisiae	FostersO			
	S. eubayanus	NCYC 1063 CDFM21L.1			
CBS 1483 group	*S. pastorianus*	CBS 1483	1087	3226	4313
	S. cerevisiae	FostersO			
	S. eubayanus	NCYC 1063 CDFM21L.1			

Saccharomyces cerevisiae-to-*Saccharomyces eubayanus* Gene Conversions Among NMT Homoeologs

To evaluate possible gene conversion among homoeologs in allopolyploid yeast, we characterized nonsynonymous SNP changes (Materials and Methods; fig. 2*A*) for single-copy NMT and non-NMT homoeologous (table 2). These changes included conversions in the *S. cerevisiae*-to-*S. eubayanus* and *S. eubayanus*-to-*S. cerevisiae* directions (*S. cerevisiae* homoeologous SNPs were converted into *S. eubayanus* homoeologous SNPs, and *vice versa*) (supplementary table S5 andS6, Supplementary Material online). We found that the percentages of *S. cerevisiae*-to-*S. eubayanus* SNPs were higher in the NMT groups than in the non-NMT groups (binomial test, P value < 0.01; fig. 2*B*) in all three allopolyploid strains. More intriguingly, a higher degree of gene conversions in the *S. cerevisiae*-to-*S. eubayanus* direction occurred in the allotriploid (CBS 1513) than in the allotetraploids (CBS 1483 and WS 34/70; binomial test, P value < 0.01; fig. 2*B*). A representative case of the NMT gene involving *Mrx15* homoeologs (encoding membrane-associated mitoribosome receptor) and its specific *S. cerevisiae*-to-*S. eubayanus* and *S. eubayanus*-to-*S. cerevisiae* gene conversions are illustrated in supplementary fig. S2*a*, Supplementary Material online, respectively. Overall, the greater *S. cerevisiae*-to-*S. eubayanus* gene conversions than the reciprocal direction in the allopolyploid *S. pastorianus* were consistent with its mtDNAs being contributed by the *S. eubayanus*-like progenitor, which implicates cytonuclear coevolution; however, more *S. cerevisiae*-to-*S. eubayanus* gene conversions in non-NMT homoeologs could be attributed to some uncharacterized selective constraint rather than cytonuclear coevolution.

To determine the extent to which gene conversions occurred in NMT homeologs, we estimated the proportion of nonsynonymous SNPs involved in gene conversions for each NMT homoeolog group, which we defined as "conversion level" (Materials and Methods; fig. 2*C*). Notably, the majority of NMT homoeologs were found to exhibit nonsynonymous *S. cerevisiae*-to-*S. eubayanus* gene conversions (*S. cerevisiae*-to-*S. eubayanus* conversion level = 1.00), meaning that all polymorphic amino acids of most *S. cerevisiae* NMT homoeologs were replaced by *S. eubayanus* amino acids (fig. 2*C*). A representative NMT homoeolog group, *PUT2*, exhibiting complete *S. cerevisiae*-to-*S. eubayanus* conversion, is illustrated in supplementary fig. S2*b*, Supplementary Material online. We note that some NMT homoeologs harbored a lower level of gene conversion or did not have any nonsynonymous *S. cerevisiae*-to-*S. eubayanus* conversions (*S. cerevisiae*-to-*S. eubayanus* conversion level = 0) (fig. 2*C*).

Temporal Transcriptional Expression Preference for *Saccharomyces eubayanus* NMT Homoeologs in *Saccharomyces pastorianus*

Cytonuclear coevolution in plant species often entails some degree of homoeologous expression bias favoring the parent contributing the allopolyploid organellar

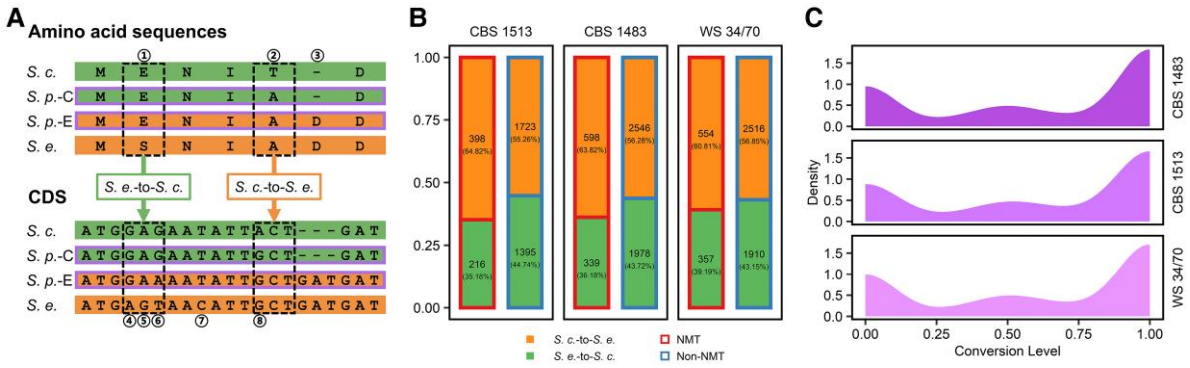

Fig. 2. Genetic cytonuclear coordination in three allopolyploid *S. pastorianus* strains. (*A*) Schematic diagram illustrating the *S. cerevisiae*-to-*S. eubayanus* (*S. c.*-to-*S. e.*) and *S. eubayanus*-to-*S. cerevisiae* (*S. e.*-to-*S. c.*) gene conversions (in right and left dotted boxes). Single-copy gene orthologs and homoeologs (C and E subgenomes) are aligned into quartets. Changes of amino acids and nucleotides involved in gene conversion are specified in each box. Labels 1-8 describe the criteria of defining nonsynonymous gene conversions among homoeologs (see Materials and Methods); (*B*) Number and relative percentage of *S. cerevisiae*-to-*S. eubayanus* (*S. c.*-to-*S. e.*) and *S. eubayanus*-to-*S. cerevisiae* (*S. e.*-to-*S. c.*) gene conversions in NMT and non-NMT homoeologs in three *S. pastorianus* strains are summarized in each column. (*C*) Density distribution of gene conversion levels of identified *S. cerevisiae*-to-*S. eubayanus* (*S. c.*-to-*S. e.*) gene conversions in each *S. pastorianus* strain.

DNAs (Adams and Wendel 2005; Gong et al. 2012, 2014; Li et al. 2020). As the unicellular allopolyploid yeast enters exponential growth in culture, there are increasing demands for energy and hence mitochondrial activity (Johnson 1968). We hypothesized that NMT homoeologs in *S. pastorianus* exhibit biased transcriptional responses consistent with selection for metabolic optimization.

To test this hypothesis (supplementary fig. S1, Supplementary Material online), we designed a microaerobic growth experiment, in which the *S. pastorianus* WS 34/70 strain was incubated for 84 h in YPD (yeast extract–peptone–dextrose) medium. Samples of mixed yeast cells were collected at intervals (three replicates at each sampling point from T1 to T37; 111 samples in total) for RNA-sequencing, covering the exponential and stationary phases (Materials and Methods; fig. 3*A*). The overall expression levels of all allotetraploid gene homoeologs were mostly similar within each growth phase, whereas among-phase expression differences were significantly higher than within-phase differences (ANOVA test, P value < 0.01; supplementary fig. S3, Supplementary Material online). Subgenomic expression of each NMT and non-NMT homoeolog pair (*S. cerevisiae* and *S. eubayanus* homoeologs) was quantified and compared for the replicates at each sampling point. The proportion of gene pairs displaying biased expression towards the *S. eubayanus* homoeolog was evaluated for NMT and non-NMT homoeolog pairs (fig. 3*B*). Of note, the extent of biased expression of *S. eubayanus* homoeologs in NMT and non-NMT homoeologs were similar throughout the stationary stage (fig. 3*B*); however, in the exponential growth phase, the number of NMT homoeolog pairs exhibiting biased expression favoring *S. eubayanus* homoeologs was significantly increased relative to that of non-NMT homoeolog pairs, which remained unchanged (fig. 3*B*).

The increased relative preference for the expression of *S. eubayanus* NMT homoeologs in the exponential phase could be attributed to the increased expression of *S. eubayanus* homoeologs and/or decreased expression of *S. cerevisiae* homoeologs. To investigate this further, we employed a method to categorize NMT homoeologs into clusters (Materials and Methods) (Abu-Jamous and Kelly 2018). The largest cluster (Cluster 0) contained 110 NMT homoeolog pairs that displayed concordant biased expression towards *S. eubayanus* homoeologs (fig. 3*C*), with most biased expression reflecting upregulation of *S. eubayanus* NMT homoeologs (ANOVA test for orthogonal contrasts, P value < 0.01; fig. 3*D*).

Compensatory Genetic and Transcriptional Cytonuclear Coordination in *Saccharomyces pastorianus* and Gene Ontology Categorization

The question arises as to whether the observed genetic and transcriptional cytonuclear responses of NMT genes in *S. pastorianus* are independent, collaborative, or compensatory. Briefly, if genetic and transcriptional cytonuclear co-evolution are independent, those responsive genes are supposed to occupy most proportion of all cytonuclear coordinative genes and be non-overlapping; if they are collaborative, there should be many common genes making both genetic and transcriptional cytonuclear co-evolutionary responses; if they are compensatory, those cytonuclear responsive genes are expected to be mutually exclusive.

To address the foregoing question, we examined the overall mutual exclusion/inclusion status of NMT genes exhibiting genetic and/or transcriptional cytonuclear responses (fig. 4), via categorizing the NMT homoeolog pairs (fig. 2*C*) into two groups according to having either high or low levels of *S. cerevisiae*-to-*S. eubayanus* gene conversions ("high" and "low"; fig. 4*A*). We also quantified expression bias toward *S. eubayanus* homoeologs at both exponential and stationary stages (fig. 4*A*). Of note, the low NMT

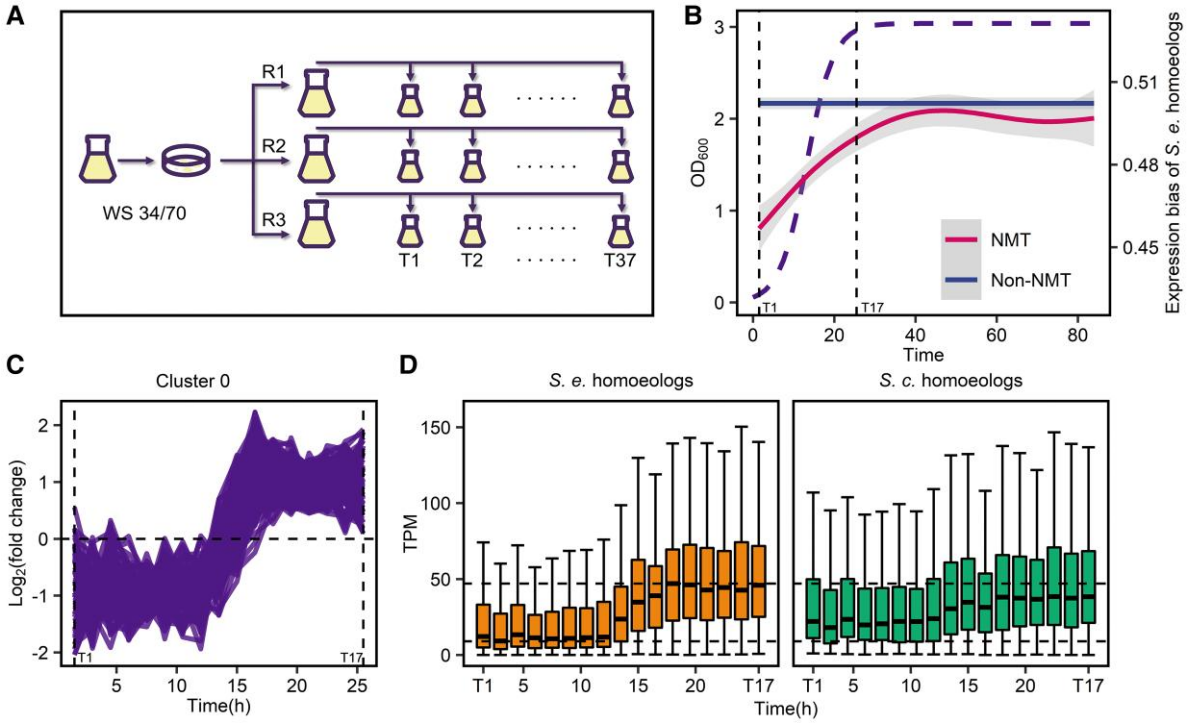

Fig. 3. Transcriptional cytonuclear coordination in *S. pastorianus* strain WS 34/70. (*A*) Microaerobic growth experiment design, in which three parallel replicates (R1 to R3) are used for sampling at each time point (T1 to T37); (*B*) Dynamic transcriptional expression bias for *S. eubayanus* homoeologs at each sampling point in the growth process. The sampling time points are denoted in *x*-axis; the absorbance value at OD_{600} for each sample and its respective expression bias of *S. eubayanus* homoeologs are denoted on the left and right *y*-axis, respectively. The dashed curve represents the growth curve; the solid curves fit the expression bias of *S. eubayanus* NMT and non-NMT genes in the time course, respectively; (*C*) The $\log_2$ transformed fold changes of transcripts per million (TPM) for NMT homoeolog pair categorized in Cluster 0; (*D*) Expression levels (TPMs) of *S. cerevisiae* and *S. eubayanus* homoeologs categorized in cluster 0 within the exponential growth phase (T1–T17 sampling points). The left and right panels represent the *S. eubayanus* and *S. cerevisiae* homoeologs, respectively. The horizontal dashed lines represent the maximum median and minimum median TPM values in all samples.

subgroup exhibited enhanced expression bias toward *S. eubayanus* homoeologs at the exponential stage, which was generally maintained until the stationary stage (fig. 4*A*); by contrast, the high NMT subgroup maintained a relatively stable homoeologous expression bias during all growth stages (fig. 4*A*).

Relative gene ontology (GO) enrichment analyses revealed that the high NMT genes were enriched in oxidoreductase activity (molecular function [MF] of GO), mitochondrial outer- and inter-membrane (cell component [CC] of GO), intrinsic components of mitochondrial membrane and envelop lumen (CC of GO), and oxidation–reduction process (biology process [BP] of GO; fig. 4*B*), whereas the low NMT genes were enriched in cytochrome complex assembly (BP of GO), mitochondrial RNA processing (BP of GO), and mitochondrial nucleoid (CC of GO; fig. 4*B*). These results indicate that the high conversion NMT genes with significant signals of gene conversion were involved in specialized mitochondrial function, concordant with cytonuclear coevolution.

To further support foregoing analysis, we determined the genetic cytonuclear status of the transcription-responsive NMT genes. Notably, most NMT genes with enhanced expression bias toward *S. eubayanus* homoeologs in Cluster 0 harbored fewer genes with complete nonsynonymous *S. cerevisiae*-to-*S. eubayanus* conversions (*S. cerevisiae*-to-*S. eubayanus* conversion level = 1.00; fig. 4*C*) than did other NMT genes. Altogether, from both viewpoints, genetic and transcriptional cytonuclear joint responses were mutually compensatory to some extent.

Discussion

Challenges faced during allopolyploid speciation involves nuclear coordination between parental subgenomes and that between nuclear and organellar genomes. As for the first challenge, loss of chromosomes and gene homoeologs and combination of subgenomic genes into one homoeolog have been characterized extensively in both plant and yeast allopolyploids (Birchler and Veitia 2012; Monerawela et al. 2015; Monerawela and Bond 2018; Salazar et al. 2019; Timouma et al. 2021; Grover et al. 2022; Birchler and Yang 2022). Another challenge is the necessity of cytonuclear coordination among divergent proteins encoded by biparental-nuclear genomes and uniparental-cytoplasmic organellar genomes. To explore the mechanisms whereby such coordination might be achieved, researchers have employed both specific organelle-targeted nuclear genes (e.g., *rbcS*, *Cox5*, and *etc.*) and/or global re-sequencing and RNA-seq data to characterize the genetic and/or transcriptional

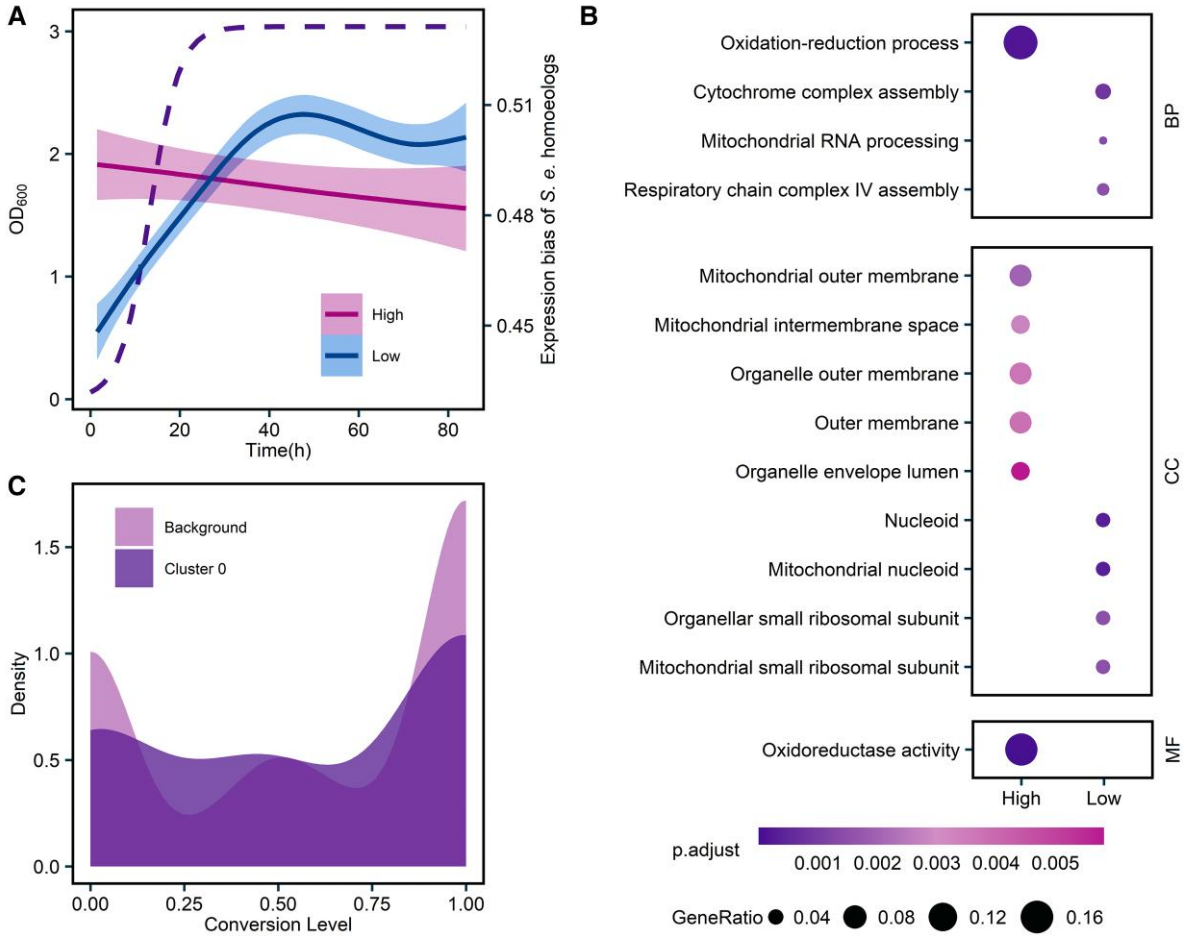

Fig. 4. Compensatory cytonuclear coordination between genetic and transcriptional responses in *S. pastorianus* strain WS 34/70. (*A*) Dynamic transcriptional expression bias for *S. eubayanus* homoeologs with high and low gene conversion levels (abbreviated as high and low at each sampling point in the growth process. The solid curves illustrate linear fitting of expression bias of *S. eubayanus* NMT homoeologs in each homoeolog group for different gene conversion levels, respectively; (*B*) GO term enrichments (biological process [BP], cellular component [CC], and molecular function [MF]) for homoeologs with high and low conversion levels (high and low). GO terms specifically enriched in homoeologous groups of high or low conversion level are specified in the diagram; (*C*) The density distribution of *S. cerevisiae*-to-*S. eubayanus* gene conversion levels for homoeologs categorized in Cluster 0 and for all other NMT genes identified in *S. pastorianus* strain (background).

cytonuclear responses in natural and synthetic allopolyploid plants (Huang et al. 2014; Sehrish et al. 2015; Roux et al. 2016; Barnard-Kubow et al. 2017; Bruun-Lund et al. 2017; Wang et al. 2017; de Carvalho Ferreira et al. 2019; Li et al. 2019, 2020; Forsythe et al. 2021; Xu et al. 2021). Nevertheless, it is still unclear to what extent optimal cytonuclear reconfigurations entail changes at genetic or transcriptional levels. To broaden our understanding of cytonuclear evolutionary processes accompanying allopolyploidy across the tree of life, the present study was conducted using the allopolyploid lager yeast *S. pastorianus*, which also allowed us to characterize cytonuclear coordination of interleaved allopolyploid yeast cells within the same population. Our findings provide novel insights into the general and unique features of cytonuclear coevolution in unicellular fungal allopolyploid species.

Gene Conversion in Nuclear Mitochondria-Targeted Genes

Mitochondria play central metabolic roles in yeast as in all aerobic organisms, but in yeast this has an economical vital function in fermentation (Kitagaki and Takagi 2014; Malina et al. 2018). The lager yeast *S. pastorianus* is known to have acquired cold tolerance (cryotolerance) from *S. eubayanus*, and hence retains its mitotype (mitochondrial DNA sequences) (Baker et al. 2015). Accordingly, *S. eubayanus*-contributed mitochondria may have been the target for natural selection in allopolyploid lager yeast favoring cytonuclear or mitonuclear interactions or function. Given the close intracellular communications between the eukaryotic nucleus and cytoplasmic organelles (Storz 2006; Quirós et al. 2016; Guaragnella et al. 2018; Malina et al. 2018), it is conceivable that selection on mtDNA also entails corresponding nuclear genomic responses. Although empirical studies have documented the occurrence of post-homoploid hybridization (hybrid at the same ploidy level) in the diploid yeast nuclear genome (Lee et al. 2008; Paliwal et al. 2014; Hsu and Chou 2017; Jhuang et al. 2017; Baker et al. 2015; Nguyen et al. 2020; Bendixsen et al. 2021), this aspect remains unexplored in allopolyploid yeast.

We propose that the data provided here constitute evidence for natural selection operating on functional cytonuclear optimization. Specifically, some specific mtDNA genes, including *cox1*, functioning in cellular respiration and mediating cryotolerance in other yeast relatives (Li et al. 2019), appear to have been under stronger purifying selection than other mtDNA genes (fig. 1*A*). We draw attention to the signals of selection were detected in NMT genes (fig. 1*B*) encoding proteins involved in mitochondrial activities. Moreover, the preferential occurrence of *S. cerevisiae*-to-*S. eubayanus* conversions in NMT homoeologs, favoring the direction of the mitochondrial genome donor, may reflect selection for optimization of function for interacting proteins encoded by mitochondrial and nuclear genes (fig. 2*B*). Specific gene homoeologs involved in the mitochondrial oxidation–reduction process (e.g. *PUT2*), exhibited complete or a high level of *S. cerevisiae*-to-*S. eubayanus* gene conversion, which we propose reflects optimization of cytonuclear function in oxidation/reduction in *S. pastorianus* (figs. 2*C*,*4B*, and supplementary fig. S2*b*, Supplementary Material online).

Further evidence is required to confirm a functional and hence possibly adaptive role for the genetic changes we report here for allopolyploid lager yeast. Taking potential participation in cryotolerance as an example, one might reverse specific *S. cerevisiae*-to-*S. eubayanus* changes by genetic engineering to study possible attenuation or abrogation of cold tolerance. In addition, it would be intriguing to elucidate the pace at which these types of evolutionary changes arise. For example, one might synthesize fast-cycling synthetic allopolyploid yeasts by mating diploid vegetative cells (Sipiczki 2008; Turgeon et al. 2021) and monitor genetic changes across generations.

Temporal Dynamics of Gene Expression and Possible Connections to Cytonuclear Function

In addition to gene conversions, duplicated genes could undergo transcriptional sub-functionalization via biased usage or expression of specific homoeologous copy (Hu et al. 2020; Nieto Feliner et al. 2020; Birchler and Yang 2022). Lager yeast cells propagated during different growth stages allows investigation of the temporal dynamics of transcriptional sub-functionalization and how it relates to possible cytonuclear selection. Here, we showed that: 1) in the early exponential growth stage, biased expression of *S. eubayanus* homoeologs for NMT genes was highest (fig. 3*B*) (Mishra and Chan 2014). The absence of these dynamics for non-NMT genes suggests a possible optimization for NMT genes during this vigorous propagation stage; 2) upon reaching the stationary phase, relatively high biased expression toward *S. eubayanus* NMT genes is maintained (fig. 3*B*), perhaps indicating a continued optimization of cytonuclear expression levels even under conditions of limited nutrition and mitotic energetic demand (Leitao and Kellogg 2017; Laman Trip and Youk 2020). Altogether, our data suggest that temporal dynamic transcriptional cytonuclear coordination could play an important fine-tuning role in the growth and propagation of allopolyploid lager yeasts. In addition, the findings of the present study suggest that allopolyploid yeasts commonly grow in an interactive and communicative manner in the same habitat, indicating that we should consider cytonuclear coordination in allopolyploids from a consolidated spatial and temporal perspective. For example, further analyses of allopolyploid lager yeasts growing in cold temperature and sampled in similar multiple growth stages will allow us to characterize the contribution of transcriptomic cytonuclear coevolution in adaptation to cold tolerance.

Genetic and Transcriptional Cytonuclear Coordination Mechanisms in Fungi and Plants

Genetic and transcriptional changes represent two different evolutionary responses that might result from selection for cytonuclear functional optimization following allopolyploidy. Conceivably, complete or high-level gene conversion (*S. cerevisiae*-to-*S. eubayanus*) of most NMT homoeologs (fig. 2*C*) became fixed early in the hybridization and/or polyploidization process, through directional selection to optimize cytonuclear function (e.g., for cryotolerance in low-temperature fermentation and/or growth habitat). As for NMT homoeologs exhibiting lower or no cytonuclear gene conversions, it is possible that this reflects either insufficient evolutionary time since the formation of the *S. pastorianus* strains, and/or the acquisition of physiological optimization via transcriptional cytonuclear responses during growth via differential transcriptional regulation of homoeologs (Johannesen and Hansen 2002; Sood et al. 2017; Hovhannisyan et al. 2020). Our findings implicate orchestrated compensatory genetic and transcriptional mechanisms to resolve cytonuclear conflict or optimize cytonuclear function.

In principle, transcriptional changes might be hypothesized to arise more quickly than genetic changes, with the latter relying on a presumably slower fixation process of favorable genome-wide mutations, whereas the former may be impacted by relatively fewer mutations in regulatory networks that might affect many genes simultaneously. In the present instance, it would be interesting to study newly synthesized allopolyploid yeasts, to determine the pace and evolutionary dynamics of expression-level changes vs. gene conversion over the generations.

As noted above, both gene conversions (in paternal-to-maternal direction) of organelle-targeted nuclear genes and biased expression for maternal homoeologs appear to be common cytonuclear responses following angiosperm allopolyploid speciation (Gong et al. 2014; Li et al. 2019, 2020). It will be interesting to explore the extent to which there are "rules" or commonalities in cytonuclear responses in allopolyploid yeasts of different ploidy levels. As the present study is the first to examine cytonuclear evolution following allopolyploidy in yeasts, it is an open question whether our findings will apply to other fungal systems, and hence how the cytonuclear evolutionary process differs or is

the same in angiosperms and fungi. We note that one aspect of our results, namely, the largely compensatory relationship between transcriptional vs. genetic alteration, has not been observed at a genome-wide scale in plant allopolyploids. It may be that this will indeed be revealed with further study, or alternatively, it is also possible that these two mechanisms often work in concert in higher plants, as exemplified by *rbcS* in some plant polyploids (Gong et al. 2012, 2014).

A final comment concerns the overall higher degree of *S. cerevisiae*-to-*S. eubayanus* gene conversion in allotriploid than allotetraploid yeast (fig. 2*B*). Perhaps this reflects the imbalance in ratios of *S. eubayanus* (mitochondrial donor) origin (1:2 and 1:1 ratios of *S. cerevisiae* vs. *S. eubayanus* homoeologous chromosomes in allotriploid and allotetraploid lager yeast, respectively), thus facilitating more frequent conversions using the extra homoeologs. Because there are plant analogs to this fungal set-up, involving unbalanced hexaploids, for example, formed via doubling of interspecific triploid intermediates, one wonders whether gene conversion will be similarly more strongly biased in these types of allopolyploid plants as they are in this single fungal system. Again, further study of multiple evolutionary systems is needed if we are to develop a general understanding of cytonuclear coevolution in polyploid eukaryotes.

Materials and Methods

Yeasts and Culture Medium

Saccharomyces pastorianus strain Weihenstephan 34/70 was obtained from China General Microbiological Culture Collection Center. The yeast was cultured in the YPD medium (w/v, 1% yeast extract, 2% peptone, and 2% D-glucose) supplemented with 100 μg/mL chloramphenicol.

Data Collection

The reference genomes of model *S. cerevisiae*, *S. eubayanus*, and *S. pastorianus* strains and re-sequencing data were downloaded from National Center for Biotechnology Information (NCBI). Strain names and respective accession numbers are tabulated in supplementary table S1, Supplementary Material online.

Genome Update and de Novo Gene Annotations

Whole-genome re-sequencing raw reads of *S. eubayanus* strain CDFM21L.1 were converted from SRA to FASTQ file format using the fastq-dump command provided by the SRA Toolkit (v2.8.0) with default filter settings (Leinonen et al. 2011). Fastp (v0.20.1) was used to filter the low-quality raw sequencing reads (Chen et al. 2018). Sambamba (v0.7.1) was used to remove PCR duplication (Tarasov et al. 2015). Clean paired reads were mapped to the reference genome (FM1318; Baker et al. 2015) using Bowtie2 (v2.4.2) with default settings (Langmead and Salzberg 2012). These data analysis pipeline were used for the other two diploid strains, *S. cerevisiae* stout strain NCYC 1063 and *S. cerevisiae* ale strain FostersO (using S288c as the reference genome; Cherry et al. 1997).

Updates for the genome assembly and annotation of our three diploid strains were obtained using RGAAT (v2.0) (Liu et al. 2018). Concerning gene annotations for *S. pastorianus* strains WS 34/70 and CBS 1513, we employed the online tool (WebAUGUSTUS, http://bioinf.uni-greifswald.de/webaugustus/; default parameters) (Stanke et al. 2006) to conduct de novo gene annotation using a training gene set from *S. pastorianus* CBS 1483 strain (Salazar et al. 2019). BUSCO (v4.1.4) was used to evaluate the completeness of genome assembly and the quality of annotations (supplementary fig. S4, Supplementary Material online) (Simão et al. 2015).

Mitochondrial genomes of *S. pastorianus* strains of CBS 1513 and WS 34/70 were de novo assembled using GetOrganelle toolkit (v1.7.5) (Jin et al. 2020). Mitochondrial genes (mtDNA genes) of *S. pastorianus* and *S. eubayanus* were predicted by the MITOS2 (v2.0.8) pipeline based on the NCBI RefSeq 89 Fungi database and using the yeast genetic code (Bernt et al. 2013).

Construction of Mitochondrial Phylogenetic Tree

To minimize the effect of AT-enrichment and long presence/absence in sequence alignment of whole-genomic mitochondrial DNAs (mtDNAs), mtDNAs of each strain were aligned with *S. cerevisiae* S288c mtDNA using Snippy (v4.6.0) in contig mode, in which core sites (genomic positions commonly shared in all strains) enclosing monomorphic nucleotide and polymorphic core SNPs will ignore the complications of long presence/absence sequences variant types and possible recombination which are frequently observed in introns and AT/GC clusters. Additionally, its contig mode also discards AT-enriched repeat regions by only maintaining regions covered by uniquely mapping reads (Seemann. T 2015). The multiple alignments were generated using MAFFT (v7.475) (Katoh and Standley 2013). A phylogenetic tree using the Neighbor-Joining method was obtained with MEGA-CC (v11) (Kumar et al. 2012), and visualized using iTOL (https://itol.embl.de/).

Prediction of Nuclear Mitochondria-Targeted Genes

Sequences of nuclear genes encoding *S. cerevisiae* proteins targeted to subcellular structures of mitochondria (mitochondrial membrane and nonmembrane) were downloaded from the fungal secretome and subcellular proteome knowledgebase (FunSecKB2, http://proteomics.ysu.edu/secretomes/fungi2/index.php) (Meinken et al. 2014). Proteins encoded by NMT genes of all yeasts in this study were identified by BLASTP (v2.6.0) against the downloaded mitochondrial subcellular protein database with similarity greater than 90%, length greater than 65%, and e-value cutoff at 10^{-12}(Camacho et al. 2009).

Calculation of the Nonsynonymous to Synonymous Substitution Ratios (d_N/d_S)

To assign the genes of *S. pastorianus* into homoeologous subgenomes (C and E), we used OrthoFinder (v2.5.2)

(default settings) (Emms and Kelly 2019) with BLASTP (v2.6.0) to compare the similarity of amino acid sequences of *S. pastorianus* genes with their two parental diploid genes. Single-copy orthogroups were identified for all yeast strains with default parameters. A single-copy orthogroup involving at least one NMT gene in a certain yeast strain was identified as a single-copy NMT group. Amino acid sequences and CDSs from the same single-copy NMT orthogroup were aligned using ParaAT (v2.0) (Zhang et al. 2012). The d_N/d_S ratio of each aligned single-copy NMT orthogroup was calculated by KaKs_Calculator package (v2.0) (Wang et al. 2010). Single-copy NMT and non-NMT orthogroups identified in *S. cerevisiae* (S288c, NCYC 1063, and FostersO strains), *S. eubayanus* (FM1318 and CDFM21L.1 strains), and *S. pastorianus* (CBS 1513, WS 34/70, and CBS 1483 strains) were input into above procedure to calculate respective d_N/d_S ratio in each diploid genome and allopolyploid subgenomes (supplementary table S3, Supplementary Material online). This method was also used for the calculation of d_N/d_S ratios for aligned mitochondrial genes (mtDNA genes) of *S. eubayanus* and *S. pastorianus*.

Identification of Nonsynonymous Homoeologous Gene Conversions Based on Homologous Gene Quartets

Subgenomic single-copy homoeologs in each allopolyploid yeast strain were aligned with their respective parental diploid orthologs identified in the same orthogroup using MAFFT (v7.475) (Katoh and Standley 2013). Single-copy gene quartets with C and E homoeologs and orthologs of *S. cerevisiae* and *S. eubayanus* were generated.

Criteria for defining nonsynonymous gene conversions among homoeologs are described below corresponding to labels 1-8 in fig. 2*A*: site 1 denotes *S. eubayanus*-to-*S. cerevisiae* amino acid conversion; site 2 indicates *S. cerevisiae*-to-*S. eubayanus* amino acid conversion; site 3 denotes a gap in the alignment that is not considered in conversion analysis; sites 4 and 5 denote the specific nucleotide changes involved in nonsynonymous *S. eubayanus*-to-*S. cerevisiae* gene conversion; site 6 indicates an automorphic nucleotide mutation occurring in an E homoeolog; site 7 denotes a synonymous substitution occurring in the E homoeolog; site 8 is a specific nucleotide change involved in *S. cerevisiae*-to-*S. eubayanus* gene conversion.

Calculation of Gene Conversion Level

Conversion level represents the proportion of *S. cerevisiae*-to-*S. eubayanus* nonsynonymous substitutions occupied in the total number of nonsynonymous substitutions in a given single-copy orthogroup, calculated as follows:

Conversion Level = (number of "*S. cerevisiae*-to-*S. eubayanus*" nonsynonymous substitutions)/(sum of all nonsynonymous substitutions). Orthogroups with conversion levels not less than 0.95 were defined as having the high conversion level, while others with conversion levels equal to or less than 0.05 were defined as the low conversion.

Microaerobic Growth Experiments

A suitable amount of *S. pastorianus* strain WS 34/70 glycerin mixture was initially drawn from a cryopreserved tube and added to 50 mL YPD liquid medium, and grown overnight in a 28°C shaker at 180 rpm to activate the strain. The cultures were evenly streaked on YPD agar plates, which were incubated upside down at 28°C until colonies appeared. Three colonies were selected as biological replications and inoculated in 30 mL YPD liquid medium, respectively. We cultured the strains overnight in a 28°C shaker with 180 rpm. For each biological replication, the yeast strain was inoculated in 37 conical flasks containing 30 mL YPD liquid medium at 1000:1 ratio. 111 conical flasks were cultured at 28°C with shaking at 180 rpm for 84 h. The cultures were sampled for OD_{600} measurements and RNA extraction at the following time points: every 1.5 h before 27 h, and every 3 h after 27 h. Three conical flasks were taken out as sample replications each time. Each sample was centrifuged at 5000 × g for 1 min at room temperature until 0.3 g yeast cells was collected in 1.5 mL microcentrifuge tube. Accordingly, yeasts were sampled at 37 time points in total for each replicate (supplementary table S4, Supplementary Material online).

RNA Extraction and Transcriptomic Sequencing

For each biological replicate, 500 µL TriPure Isolation Reagent (Roche Diagnostics GmbH, Mannheim, Germany) and 0.3 g acid-washed glass beads (SIGMA, USA) rapidly were added. After vibrating on the vortex oscillator at the maximum speed for 1 min, samples were put into liquid nitrogen for rapid freezing. This freezing and thawing vibration was repeated five times. After complete melting, the tube was incubated on ice for 5 min to lyse the yeast cells. The total RNA was purified using UNIQ-10 Column Trizol Total RNA Isolation Kit (Sangon Biotech, Shanghai, China).

RNA was treated by DNase I and purified using the RNA clean Kit (Qiagen, Germany). High-quality RNA was used for the subsequent library constructions. Ribosomal RNA (rRNA) was removed by Epicentre Ribo-zeroTM rRNA Removal Kit (Epicentre, USA), and rRNA free residue was cleaned up by ethanol precipitation. Strand-specific sequencing libraries were constructed by the NEBNext Ultra Directional RNA Library Prep Kit for Illumina (NEB, USA). The resulting library was sequenced on the Illumina Nova 6000 platform in PE150 bp mode at the Novogene Company (Beijing, China).

Differentially Expressed Genes Analysis

Fastp (v0.20.1) was used to filter the low-quality raw sequencing reads (Chen et al. 2018). The reads from ribosome RNA were removed using Bowtie2 (v2.4.2) (Langmead and Salzberg 2012) based on SILVA (https://www.arb-silva.de/) (Quast et al. 2012) and Pfam (Mistry

et al. 2021). Clean reads were mapped to the *S. pastorianus* strain WS 34/70 reference genome (Okuno et al. 2016) using HISAT2 (v2.2.1) (Kim et al. 2019). The reads counts of each sample were quantified by featureCounts (v2.0.1) with the parameters set as "-p -s 2" (Liao et al. 2014). Differentially expressed genes (DEGs) in two subgenomes (*S. eubayanus* homoeologs as the numerator and *S. cerevisiae* homoeologs as the denominator) were identified using DESeq2 (v1.30.1) based on false discovery rate adjusted P value < 0.05. Clust (v1.12.0) was employed to cluster the subgenomic DEGs in terms of their similarity in expression pattern in the temporal course of the lag and exponential phases (T1 to T17) (Abu-Jamous and Kelly 2018).

Gene Ontology Analysis

GO term enrichment analysis was performed using the compareCluster command provided by the R package clusterProfiler (v3.18.1). All genes of *S. pastorianus* strain WS 34/70 were used as the reference background.

Calculation of Transcriptional Expression Bias for *Saccharomyces eubayanus* Homoeologs

The proportion of highly expressed *S. eubayanus* homoeologs was calculated as follows:

Transcriptional expression preference for *S. eubayanus* NMT homoeologs = (Number of groups with significantly higher expression in *S. eubayanus* homoeologs)/(Sum of total DEGs groups).

Supplementary Material

Supplementary data are available at *Molecular Biology and Evolution* online.

Acknowledgments

We thank Fengyan Bai for sharing the yeast strains used in this study. We also appreciate the knowledge and training given by the course of Evolution Biology in Northeast Normal University.

Author Contributions

Conceptualization: B.L. and L.G., Methodology: Z.Z. and T.W., Investigation: K.Z., J.L., G.L. and Y.Z., Experiments: K.Z., J.L., Y.Z., W.S., J.W. J.Y. and Y.M., Data Analysis: K.Z., J.L., Y.Do. and H.W., Supervision: L.G., Writing—original draft: K.Z. and J.L., Writing—review & editing: J.F.W., B.L., and L.G.

Funding

This work was supported by the Joint National Natural Science Foundation of China (NSFC) and the Israel Science Foundation (ISF) research program (32061143001).

Data Availability

RNA-sequencing data have been deposited and are available in the NCBI (PRJNA808674). All other data are available in the paper and/or the Supplementary files.

References

Abu-Jamous B, Kelly S. 2018. Clust: automatic extraction of optimal co-expressed gene clusters from gene expression data. *Genome Biol.* **19**:1–11.

Adams KL, Wendel JF. 2005. Novel patterns of gene expression in polyploid plants. *Trends Genet.* **21**:539–543.

Albertin W, Marullo P. 2012. Polyploidy in fungi: evolution after whole-genome duplication. *Proc Biol Sci.* **279**:2497–2509.

Angelika BH, Opalińska M, Gerbeth C, Herman Josip S, Rao S, Schönfisch B, Guiard B, Schmidt O, Pfanner N, Meisinger C. 2014. Cell cycle-dependent regulation of mitochondrial preprotein translocase. *Science.* **346**:1109–1113.

Baker EmilyClare P, Wang B, Bellora N, Peris D, Hulfachor AB, Koshalek JA, Adams M, Libkind D, Hittinger CT. 2015. The genome sequence of *Saccharomyces eubayanus* and the domestication of lager-brewing yeasts. *Mol Biol Evol.* **32**:2818–2831.

Barnard-Kubow KB, McCoy MA, Galloway LF. 2017. Biparental chloroplast inheritance leads to rescue from cytonuclear incompatibility. *New Phytol.* **213**:1466–1476.

Bendixsen DP, Peris D, Stelkens R. 2021. Patterns of genomic instability in interspecific yeast hybrids with diverse ancestries. *Front Fungal Biol.* **2**:52.

Bernt M, Donath A, Jühling F, Externbrink F, Florentz C, Fritzsch G, Pütz J, Middendorf M, Stadler PF. 2013. MITOS: improved de novo metazoan mitochondrial genome annotation. *Mol Phylogenet Evol.* **69**:313–319.

Bing J, Han PJ, Liu WQ, Wang QM, Bai FY. 2014. Evidence for a far East Asian origin of lager beer yeast. *Curr Biol.* **24**:R380–R381.

Birchler JA, Veitia RA. 2012. Gene balance hypothesis: connecting issues of dosage sensitivity across biological disciplines. *Proc Natl Acad Sci U S A.* **109**:14746–14753.

Birchler JA, Yang H. 2022. The multiple fates of gene duplications: deletion, hypofunctionalization, subfunctionalization, neofunctionalization, dosage balance constraints, and neutral variation. *Plant Cell.* **34**:2466–2474.

Bleoanca I, Silva ARC, Pimentel C, Rodrigues-Pousada C, Menezes Rde A. 2013. Relationship between ethanol and oxidative stress in laboratory and brewing yeast strains. *J Biosci Bioeng.* **116**:697–705.

Bousquet I, Dujardin G, Slonimski PP. 1991. ABC1, a novel yeast nuclear gene has a dual function in mitochondria: it suppresses a cytochrome b mRNA translation defect and is essential for the electron transfer in the bc 1 complex. *EMBO J.* **10**:2023–2031.

Bruun-Lund S, Clement WL, Kjellberg F, Rønsted N. 2017. First plastid phylogenomic study reveals potential cyto-nuclear discordance in the evolutionary history of *Ficus* L. (Moraceae). *Mol Phylogenet Evol.* **109**:93–104.

Camacho C, Coulouris G, Avagyan V, Ma N, Papadopoulos J, Bealer K, Madden TL. 2009. BLAST+: architecture and applications. *BMC Bioinformatics.* **10**:421.

Chen S, Zhou Y, Chen Y, Gu J. 2018. fastp: an ultra-fast all-in-one FASTQ preprocessor. *Bioinformatics.* **34**:i884–i890.

Cherry JM, Ball C, Weng S, Juvik G, Schmidt R, Adler C, Dunn B, Dwight S, Riles L, Mortimer RK. 1997. Genetic and physical maps of *Saccharomyces cerevisiae*. *Nature.* **387**:67.

Choleva L, Janko K. 2013. Rise and persistence of animal polyploidy: evolutionary constraints and potential. *Cytogenet Genome Res.* **140**:151–170.

de Carvalho JF, Lucas J, Deniot G, Falentin C, Filangi O, Gilet M, Legeai F, Lode M, Morice J, Trotoux G, *et al.* 2019. Cytonuclear interactions remain stable during allopolyploid evolution despite

repeated whole-genome duplications in Brassica. *Plant J*. **98**: 434–447.
EmilyClare PB, Peris D, Moriarty Ryan V, Li Xueying C, Fay Justin C, Hittinger Chris T. 2019. Mitochondrial DNA and temperature tolerance in lager yeasts. *Sci Adv*. **5**:eaav1869.
Emms DM, Kelly S. 2019. OrthoFinder: phylogenetic orthology inference for comparative genomics. *Genome Biol*. **20**:1–14.
Forsythe ES, Grover CE, Miller ER, Conover JL, Arick MA, Chavarro MCF, Leal-Bertioli SCM, Peterson DG, Sharbrough J, Wendel JF, *et al*. 2022. Organellar transcripts dominate the cellular mRNA pool across plants of varying ploidy levels. *Proc Natl Acad Sci U S A*. **119**:e2204187119.
Forsythe ES, Williams AM, Sloan DB. 2021. Genome-wide signatures of plastid-nuclear coevolution point to repeated perturbations of plastid proteostasis systems across angiosperms. *Plant Cell*. **33**:980–997.
Ginovart M, Carbó R, Blanco M, Portell X. 2018. Digital image analysis of yeast single cells growing in two different oxygen concentrations to analyze the population growth and to assist individual-based modeling. *Front Microbiol*. **8**.
Ginovart M, Prats C, Portell X, Silbert M. 2011. Exploring the lag phase and growth initiation of a yeast culture by means of an individual-based model. *Food Microbiol*. **28**:810–817.
Gong L, Olson M, Wendel JF. 2014. Cytonuclear evolution of Rubisco in four allopolyploid lineages. *Molecular Biology and Evolution*. **31**:2624–2636.
Gong L, Salmon A, Yoo MJ, Grupp KK, Wang Z, Paterson AH, Wendel JF. 2012. The cytonuclear dimension of allopolyploid evolution: an example from cotton using Rubisco. *Mol Biol Evol*. **29**:3023–3036.
Gorkovskiy A, Verstrepen KJ. 2021. The role of structural variation in adaptation and evolution of yeast and other fungi. *Genes*. **12**:699.
Grover CE, Forsythe ES, Sharbrough J, Miller ER, Conover JL, DeTar RA, Chavarro C, Arick MA II, Peterson DG, Leal-Bertioli SCM, *et al*. 2022. Variation in cytonuclear expression accommodation among allopolyploid plants. *Genetics*. **222**:iyac118.
Guaragnella N, Coyne LP, Chen XJ, Giannattasio S. 2018. Mitochondria–cytosol–nucleus crosstalk: learning from *Saccharomyces cerevisiae*. *FEMS Yeast Res*. **18**:foy088.
Hovhannisyan H, Saus E, Ksiezopolska E, Hinks Roberts AJ, Louis EJ, Gabaldón T. 2020. Integrative omics analysis reveals a limited transcriptional shock after yeast interspecies hybridization. *Front Genet*. **11**:404.
Hsu YY, Chou JY. 2017. Environmental factors can influence mitochondrial inheritance in the *Saccharomyces* yeast Hybrids. *PLoS One*. **12**:e0169953.
Hu G, Grover CE, Arick MA, Liu M, Peterson DG, Wendel JF. 2020. Homoeologous gene expression and co-expression network analyses and evolutionary inference in allopolyploids. *Brief Bioinform*. **22**:1819–1835.
Huang DI, Hefer CA, Kolosova N, Douglas CJ, Cronk QCB. 2014. Whole plastome sequencing reveals deep plastid divergence and cytonuclear discordance between closely related balsam poplars, *Populus balsamifera* and *P. trichocarpa* (Salicaceae). *New Phytol*. **204**:693–703.
Jhuang HY, Lee HY, Leu JY. 2017. Mitochondrial–nuclear coevolution leads to hybrid incompatibility through pentatricopeptide repeat proteins. *EMBO Rep*. **18**:87–101.
Jiao Y, Wickett NJ, Ayyampalayam S, Chanderbali AS, Landherr L, Ralph PE, Tomsho LP, Hu Y, Liang H, Soltis PS, *et al*. 2011. Ancestral polyploidy in seed plants and angiosperms. *Nature*. **473**:97–100.
Jin JJ, Yu WB, Yang JB, Song Y, dePamphilis CW, Yi TS, Li DZ. 2020. GetOrganelle: a fast and versatile toolkit for accurate de novo assembly of organelle genomes. *Genome Biol*. **21**:241.
Johannesen PF, Hansen J. 2002. Differential transcriptional regulation of sulfur assimilation gene homologues in the Saccharomyces carlsbergensis yeast species hybrid. *FEMS Yeast Res*. **1**:315–322.
Johnson BF. 1968. Morphometric analysis of yeast cells: II. Cell size of *Schizosaccharomyces pombe* during the growth cycle. *Exp Cell Res*. **49**:59–68.
Katoh K, Standley DM. 2013. MAFFT multiple sequence alignment software version 7: improvements in performance and usability. *Mol Biol Evol*. **30**:772–780.
Kim D, Paggi JM, Park C, Bennett C, Salzberg SL. 2019. Graph-based genome alignment and genotyping with HISAT2 and HISAT-genotype. *Nat Biotechnol*. **37**:907–915.
Kitagaki H, Takagi H. 2014. Mitochondrial metabolism and stress response of yeast: applications in fermentation technologies. *J Biosci Bioeng*. **117**:383–393.
Krogerus K, Arvas M, De Chiara M, Magalhães F, Mattinen L, Oja M, Vidgren V, Yue JX, Liti G, Gibson B. 2016. Ploidy influences the functional attributes of de novo lager yeast hybrids. *Appl Microbiol Biotechnol*. **100**:7203–7222.
Kumar S, Stecher G, Peterson D, Tamura K. 2012. MEGA-CC: computing core of molecular evolutionary genetics analysis program for automated and iterative data analysis. *Bioinformatics*. **28**: 2685–2686.
Laman Trip DS, Youk H. 2020. Yeasts collectively extend the limits of habitable temperatures by secreting glutathione. *Nat Microbiol*. **5**:943–954.
Langmead B, Salzberg SL. 2012. Fast gapped-read alignment with Bowtie 2. *Nat Methods*. **9**:357–359.
Leducq JB, Henault M, Charron G, Nielly-Thibault L, Terrat Y, Fiumera HL, Shapiro BJ, Landry CR. 2017. Mitochondrial recombination and introgression during speciation by hybridization. *Mol Biol Evol*. **34**:1947–1959.
Lee HY, Chou JY, Cheong L, Chang NH, Yang SY, Leu JY. 2008. Incompatibility of nuclear and mitochondrial genomes causes hybrid sterility between two yeast species. *Cell*. **135**:1065–1073.
Leinonen R, Sugawara H, Shumway M. 2011. The sequence read archive. *Nucleic Acids Res*. **39**:D19–D21.
Leitao RM, Kellogg DR. 2017. The duration of mitosis and daughter cell size are modulated by nutrients in budding yeast. *J Cell Biol*. **216**:3463–3470.
Li XC, Peris D, Hittinger CT, Sia EA, Fay JC. 2019b. Mitochondria-encoded genes contribute to evolution of heat and cold tolerance in yeast. *Sci Adv*. **5**:eaav1848.
Li C, Sun X, Conover JL, Zhang Z, Wang J, Wang X, Deng X, Wang H, Liu B, Wendel JF, *et al*. 2019a. Cytonuclear coevolution following homoploid hybrid speciation in *Aegilops tauschii*. *Mol Biol Evol*. **36**:341–349.
Li C, Wang X, Xiao Y, Sun X, Wang J, Yang X, Sun Y, Sha Y, Lv R, Yu Y, *et al*. 2020. Coevolution in hybrid genomes: nuclear-encoded rubisco small subunits and their plastid-targeting translocons accompanying sequential allopolyploidy events in triticum. *Mol Biol Evol*. **37**:3409–3422.
Liao Y, Smyth GK, Shi W. 2014. featureCounts: an efficient general purpose program for assigning sequence reads to genomic features. *Bioinformatics*. **30**:923–930.
Libkind D, Hittinger CT, Valério E, Gonçalves C, Dover J, Johnston M, Gonçalves P, Sampaio JP. 2011. Microbe domestication and the identification of the wild genetic stock of lager-brewing yeast. *Proc Natl Acad Sci U S A*. **108**:14539–14544.
Liu W, Wu S, Lin Q, Gao S, Ding F, Zhang X, Aljohi HA, Yu J, Hu S. 2018. RGAAT: a reference-based genome assembly and annotation tool for new genomes and upgrade of known genomes. *Genomics Proteomics Bioinformatics*. **16**:373–381.
MacLean RC, Gudelj I. 2006. Resource competition and social conflict in experimental populations of yeast. *Nature*. **441**: 498–501.
Malina C, Larsson C, Nielsen J. 2018. Yeast mitochondria: an overview of mitochondrial biology and the potential of mitochondrial systems biology. *FEMS Yeast Res*. **18**(05):foy040.
Marsit S, Hénault M, Charron G, Fijarczyk A, Landry CR. 2021. The neutral rate of whole-genome duplication varies among yeast species and their hybrids. *Nat Commun*. **12**:1–11.
Meinken J, Asch DK, Neizer-Ashun KA, Chang GH, R.Cooper JRC, Min XJ. 2014. FunSecKB2: a fungal protein subcellular location knowledgebase. *Comput Mol Biol*. **4**:1492.

Mishra P, Chan DC. 2014. Mitochondrial dynamics and inheritance during cell division, development and disease. *Nat Rev Mol Cell Biol*. **15**:634–646.

Mistry J, Chuguransky S, Williams L, Qureshi M, Salazar GA, Sonnhammer ELL, Tosatto SCE, Paladin L, Raj S, Richardson LJ, *et al*. 2021. Pfam: the protein families database in 2021. *Nucleic Acids Res*. **49**:D412–D419.

Monerawela C, Bond U. 2018. The hybrid genomes of *Saccharomyces pastorianus*: a current perspective. *Yeast*. **35**:39–50.

Monerawela C, James TC, Wolfe KH, Bond U. 2015. Loss of lager specific genes and subtelomeric regions define two different *Saccharomyces cerevisiae* lineages for *Saccharomyces pastorianus* group I and II strains. *FEMS Yeast Res*. **15**(02):fou008.

Nakao Y, Kanamori T, Itoh T, Kodama Y, Rainieri S, Nakamura N, Shimonaga T, Hattori M, Ashikari T. 2009. Genome sequence of the lager brewing yeast, an interspecies hybrid. *DNA Res*. **16**: 115–129.

Nguyen THM, Sondhi S, Ziesel A, Paliwal S, Fiumera HL. 2020. Mitochondrial-nuclear coadaptation revealed through mtDNA replacements in *Saccharomyces cerevisiae*. *BMC Evol Biol*. **20**:128.

Nieto Feliner G, Casacuberta J, Wendel JF. 2020. Genomics of evolutionary novelty in hybrids and polyploids. *Front Genet*. **11**: 792.

Okuno M, Kajitani R, Ryusui R, Morimoto H, Kodama Y, Itoh T. 2016. Next-generation sequencing analysis of lager brewing yeast strains reveals the evolutionary history of interspecies hybridization. *DNA Res* **23**(01):67–80.

Olivares-Marin IK, González-Hernández JC, Regalado-Gonzalez C, Madrigal-Perez LA. 2018. *Saccharomyces cerevisiae* exponential growth kinetics in batch culture to analyze respiratory and fermentative metabolism. *J Vis Exp*:e58192.

Paliwal S, Fiumera AC, Fiumera HL. 2014. Mitochondrial-nuclear epistasis contributes to phenotypic variation and coadaptation in natural isolates of *Saccharomyces cerevisiae*. *Genetics*. **198**: 1251–1265.

Quast C, Pruesse E, Yilmaz P, Gerken J, Schweer T, Yarza P, Peplies J, Glöckner FO. 2012. The SILVA ribosomal RNA gene database project: improved data processing and web-based tools. *Nucleic Acids Res*. **41**:D590–D596.

Quirós PM, Mottis A, Auwerx J. 2016. Mitonuclear communication in homeostasis and stress. *Nat Rev Mol Cell Biol*. **17**: 213–226.

Rodriguez F, Arkhipova IR. 2018. Transposable elements and polyploid evolution in animals. *Curr Opin Genet Dev*. **49**:115–123.

Roux F, Mary-Huard T, Barillot E, Wenes E, Botran L, Durand S, Villoutreix R, Martin-Magniette M-L, Camilleri C, Budar F. 2016. Cytonuclear interactions affect adaptive traits of the annual plant *Arabidopsis thaliana* in the field. *Proc Natl Acad Sci U S A*. **113**:3687.

Salazar AN, de Vries ARG, van den Broek M, Brouwers N, de la Torre Cortès P, Kuijpers NGA, Daran JMG, Abeel T. 2019. Chromosome level assembly and comparative genome analysis confirm lager-brewing yeasts originated from a single hybridization. *BMC Genomics*. **20**:916.

Scott AL, Richmond PA, Dowell RD, Selmecki AM. 2017. The influence of polyploidy on the evolution of yeast grown in a suboptimal carbon source. *Mol Biol Evol*. **34**:2690–2703.

Seemann T. 2015. Snippy: rapid haploid variant calling; [accessed 2022 Sep 3]. https://github.com/tseemann/snippy.

Sehrish T, Symonds VV, Soltis DE, Soltis PS, Tate JA. 2015. Cytonuclear coordination is not immediate upon allopolyploid formation in T*ragopogon miscellus* (Asteraceae) allopolyploids. *PLoS One*. **10**:e0144339.

Selmecki AM, Maruvka YE, Richmond PA, Guillet M, Shoresh N, Sorenson AL, De S, Kishony R, Michor F, Dowell R, *et al*. 2015. Polyploidy can drive rapid adaptation in yeast. *Nature*. **519**: 349–352.

Sharbrough J, Conover JL, Fernandes Gyorfy M, Grover CE, Miller ER, Wendel JF, Sloan DB. 2022. Global patterns of subgenome evolution in organelle-targeted genes of six allotetraploid angiosperms. *Mol Biol Evol*. **39**:msac074.

Simão FA, Waterhouse RM, Ioannidis P, Kriventseva EV, Zdobnov EM. 2015. BUSCO: assessing genome assembly and annotation completeness with single-copy orthologs. *Bioinformatics*. **31**: 3210–3212.

Sipiczki M. 2008. Interspecies hybridization and recombination in *Saccharomyces* wine yeasts. *FEMS Yeast Res*. **8**:996–1007.

Sloan DB, Warren JM, Williams AM, Wu Z, Abdel-Ghany SE, Chicco AJ, Havird JC. 2018. Cytonuclear integration and co-evolution. *Nat Rev Genet*. **19**:635–648.

Solieri L. 2010. Mitochondrial inheritance in budding yeasts: towards an integrated understanding. *Trends Microbiol*. **18**:521–530.

Soltis PS, Marchant DB, Van de Peer Y, Soltis DE. 2015. Polyploidy and genome evolution in plants. *Curr Opin Plant Biol*. **35**: 119–125.

Sood V, Cajigas I, D'Urso A, Light WH, Brickner JH. 2017. Epigenetic transcriptional memory of GAL genes depends on growth in glucose and the Tup1 transcription factor in *Saccharomyces cerevisiae*. *Genetics*. **206**:1895–1907.

Stanke M, Keller O, Gunduz I, Hayes A, Waack S, Morgenstern B. 2006. AUGUSTUS: ab initio prediction of alternative transcripts. *Nucleic Acids Res*. **34**:W435–W439.

Storz P. 2006. Reactive oxygen species–mediated mitochondria-to-nucleus signaling: a key to aging and radical-caused diseases. *Sci STKE*. **2006**:re3.

Tarasov A, Vilella AJ, Cuppen E, Nijman IJ, Prins P. 2015. Sambamba: fast processing of NGS alignment formats. *Bioinformatics*. **31**: 2032–2034.

Timouma S, Balarezo-Cisneros LN, Pinto J, De La Cerda R, Bond U, Schwartz JM, Delneri D. 2021. Transcriptional profile of the industrial hybrid *Saccharomyces pastorianus* reveals temperature-dependent allele expression bias and preferential orthologous protein assemblies. *Mol Biol Evol*. **38**:5437–5452.

Todd Robert T, Forche A, Selmecki A, Heitman J, Stukenbrock Eva H. 2017. Ploidy variation in fungi: polyploidy, aneuploidy, and genome evolution. *Microbiol Spectr*. **5**.

Turgeon Z, Sierocinski T, Brimacombe CA, Jin Y, Goldhawke B, Swanson JM, Husnik JI, Dahabieh MS. 2021. Industrially applicable de novo lager yeast Hybrids with a unique genomic architecture: creation and characterization. *Appl Environ Microbiol*. **87**: e02434-20.

Wang X, Dong Q, Li X, Yuliang A, Yu Y, Li N, Liu B, Gong L. 2017. Cytonuclear variation of Rubisco in synthesized rice hybrids and allotetraploids. *Plant Genome*. **10**.

Wang D, Zhang Y, Zhang Z, Zhu J, Yu J. 2010. KaKs_Calculator 2.0: a toolkit incorporating gamma-series methods and sliding window strategies. *Genomics Proteomics Bioinformatics*. **8**:77–80.

Wu CH, Huang CH, Chung MC, Chang SH, Tsai GJ. 2021. Exploration of hypoglycemic activity of *Saccharomyces pastorianus* extract and evaluation of the molecular mechanisms. *Molecules*. **26**.

Xu LL, Yu RM, Lin XR, Zhang BW, Li N, Lin K, Zhang DY, Bai WN. 2021. Different rates of pollen and seed gene flow cause branch-length and geographic cytonuclear discordance within Asian butternuts. *New Phytol*. **232**:388–403.

Youk H, Lim Wendell A. 2014. Secreting and sensing the same molecule allows cells to achieve versatile social behaviors. *Science*. **343**:1242782.

Zhang Z, Xiao J, Wu J, Zhang H, Liu G, Wang X, Dai L. 2012. ParaAT: a parallel tool for constructing multiple protein-coding DNA alignments. *Biochem Biophys Res Commun*. **419**:779–781.